ISSN:1984-2295

Revista Brasileira de Geografia Física

Homepage:https://periodicos.ufpe.br/revistas/rbgfe

Effects of Spatial Resolution on Topographic Representations and Drainage Networks Derived from LiDAR Digital Terrain Model

Rafael Carneiro de Souza Barros[1], Adriano Rolim da Paz[1]

[1]Graduate Program in Civil and Environmental Engineering – Federal University of Paraíba (UFPB, Campus I Lot. Cidade Universitária, ZIP code 58051900, Joao Pessoa/PB, rafaelhc3@gmail.com (https://orcid.org/0000-0003-3214-2292), adrianorpaz@yahoo.com.br (https://orcid.org/0000-0002-2479-4461); Corresponding author: rafaelhc3@gmail.com (https://orcid.org/0000-0003-3214-2292)

Modelos Digitais de Terreno (MDT) derivados da tecnologia LiDAR estão cada vez mais disponíveis. Porém, trabalhar com esses MDT s acarreta altos custos computacionais e exige equipamentos de alto desempenho, o que pode até inviabilizar a utilização desses modelos. O objetivo deste trabalho é avaliar os efeitos causados pela alteração da resolução espacial em representações topográficas e redes de drenagem extraídas do LiDAR-MDT. Para isso, foram aplicadas três técnicas de reamostragem, agregação média, interpolação bilinear e interpolação do vizinho mais próximo, para tornar grosseiro um LiDAR- MDT de resolução espacial de 1 m em múltiplas resoluções (2, 10, 30 e 100 m). Uma sub-bacia (550 km²) da bacia do Rio Sirinhaém foi tomada como área de estudo de caso. Os resultados mostram que não houve diferença significativa entre as técnicas de reamostragem, mas sim entre as resoluções espaciais, variando de acordo com a métrica aplicada. A resolução espacial de 2 m é mais adequada caso seja necessária uma resolução mais grosseira.

Artigo recebido em 16/01/2024 e aceito em 03/06/2024

A B S T R A C T

Digital Terrain Models (DTM) derived from LiDAR technology are increasingly available. However, working with these DTMs causes high computational costs and requires high-performance equipment, which may even make the use of these models unfeasible. The objective of this work is to evaluate the effects caused by changing spatial resolution in topographic representations and drainage networks extracted from LiDAR-DTM. For this, three resampling techniques were applied, mean aggregation, bilinear interpolation and nearest neighbor interpolation, to coarse a 1 m spatial resolution LiDAR-DTM in multiple resolutions (2, 10, 30 and 100 m). A sub-basin (550 km²) of the Sirinhaem River basin was taken as the case study area. The results show that there was no significant difference between the resampling techniques, but between the spatial resolutions, varying according to the applied metric. The spatial resolution of 2 m is more suitable in case of the need for a coarser resolution.

Keywords: Resampling; Computational cost; Digital elevation model.

Efeitos da Resolução Espacial nas Representações Topográficas e Redes de Drenagem Derivadas de Modelo Digital de Terreno LiDAR

R E S U M O

Modelos Digitais de Terreno (MDT) derivados da tecnologia LiDAR estão cada vez mais disponíveis. Porém, trabalhar com esses MDT s acarreta altos custos computacionais e exige equipamentos de alto desempenho, o que pode até inviabilizar a utilização desses modelos. O objetivo deste trabalho é avaliar os efeitos causados pela alteração da resolução espacial em representações topográficas e redes de drenagem extraídas do LiDAR-MDT. Para isso, foram aplicadas três técnicas de reamostragem, agregação média, interpolação bilinear e interpolação do vizinho mais próximo, para tornar grosseiro um LiDAR- MDT de resolução espacial de 1 m em múltiplas resoluções (2, 10, 30 e 100 m). Uma sub-bacia (550 km²) da bacia do Rio Sirinhaém foi tomada como área de estudo de caso. Os resultados mostram que não houve diferença significativa entre as técnicas de reamostragem, mas sim entre as resoluções espaciais, variando de acordo com a métrica aplicada. A resolução espacial de 2 m é mais adequada caso seja necessária uma resolução mais grosseira.

Palavras-chave: Reamostragem, Custo computacional, Modelo Digital de Elevação.

Introduction

The use of Digital Terrain Models (DTMs) is of great value for a range of environmental studies. Over the last decade, several DTM products have become publicly available, expanding their application in research and contributing significantly to the theme of water resources (Woodrow et al., 2016).

DTMs are frequently employed for environmental management purposes, providing crucial information for mapping natural resources and natural disasters influenced by topography.

They play a significant role in various predictive models for public utility, such as climate models, rainfall-runoff models, and flood estimation and propagation models (Roostaee & Deng, 2023).

Currently, there are diverse DTM products, ranging from high spatial resolution and precision ones, for example, derived from Light Detection and Ranging (LiDAR) technology, to global survey products like Advanced Spaceborne Thermal Emission and Reflection Radiometer (ASTER), Shuttle Radar Topography Mission (SRTM), and Advanced Land Observing Satellite (ALOS) (Azizian & Brocca, 2020).

The increased availability of LiDAR-derived Digital Terrain Models (DTMs) has led to a rise in the number of studies aiming to explore the comparison of this type of DTM with widely used global surveys, such as SRTM. These comparisons typically assess which model can deliver products with greater accuracy concerning topographic and hydrological parameters (Persendt & Gomez, 2016).

The acquisition of LiDAR-derived DTMs is generally justified by the high level of detail in the product (Lindsay et al., 2019). This type of product usually has spatial resolutions ranging from a few centimeters to 3 meters (Muhadi et al., 2020). Therefore, LiDAR-derived DTMs can represent small variations in topography, adding greater complexity to the model. This may be undesirable as it impacts topographic characterization and complicates the estimation of geomorphological indices such as slope and flow directions (Lindsay & Creed, 2005; Lindsay et al., 2019).

Although the use of LiDAR-derived Digital Terrain Models (DTMs) has increased, their availability is still limited due to the high acquisition cost and technical challenges in data acquisition and processing (Zhang et al., 2019). For developing countries, for instance, there are both financial and practical challenges associated with handling LiDAR-derived DTMs for large areas. This makes higher spatial resolution not necessarily the most appropriate, given the high computational processing cost. It becomes preferable to work with DTMs of spatial resolution suitable for processing capacity and the size of the study area (Muthusamy et al., 2021).

Therefore, one alternative for working with DTMs of suitable spatial resolution is to resample LiDAR-derived DTMs to a coarser spatial resolution. Resampling allows defining an intermediate resolution between coarse and fine resolutions, providing a level of detail that offers adequate information density and minimizing processing time according to the chosen objective (Winzeler et al., 2022).

Research indicates that due to limitations such as computational capacity, algorithm processing time, and the large disk size of original LiDAR data, LiDAR-derived Digital Terrain Models (DTMs) can be resampled to coarser resolutions to enable the extraction of hydrological and geomorphological features at desired scales (Persendt & Gomez, 2016).

Resampling LiDAR-derived DTMs to coarser resolutions becomes essential to make these models usable on medium to low-performance computers, in large study areas, and for data integration with coarser spatial resolution products (Le Coz et al., 2009). Furthermore, the simplification induced by resampling can benefit management efforts, allowing faster and less costly operations of mathematical models at watershed scales. The results of these operations facilitate the work of managers by providing prioritized and quicker decision-making (Lisenby & Fryirs, 2017).

Several studies in different areas have evaluated the effects caused by the application of different resampling techniques in DTM-LiDAR and show that the performance of each technique can vary according to the degraded spatial resolution and the analyzed information plan (Goulden et al., 2014; Meles et al., 2020; Erdbrugger et al., 2021; Muthusamy et al., 2021; Sliwinski et al., 2022).

To illustrate this, previous works show that resampling DTM-LiDAR to coarser resolutions impacts different topographic indices. For example, it affects the estimation of slope values and results in the underestimation of contributing areas, flow path lengths, and the drainage network of watersheds (Sorensen & Seinert, 2007; Goulden et al., 2014; Woodrow et al., 2016; Erdbrugger et al., 2021).

It is also reported that, with an increase in the degree of spatial resolution coarsening, the elimination of topographic features occurs, slope values decrease, hydrography simplifies in complex surfaces, and there is an overestimation of hydrological connectivity and surface runoff, along with a significant reduction in computational cost (Le Coz et al., 2009; Yang & Chu, 2013; Grohmann, 2015; Habtezion et al., 2016; Muthusamy et al., 2021;).

The loss of information caused by the coarsening of spatial resolution can lead to errors in DTM-derived products and consequently affect other information plans. For example, errors in DTM-derived products such as watershed

delineation, river length, flow paths, and drainage network can negatively impact the calculation of the water balance of watersheds, representation of flood waves, sediment and pollutant transport, and groundwater recharge (De Sousa & Paz, 2017).

In this sense, LiDAR-derived Digital Terrain Models (DTM-LiDAR) represent an innovative product with significant potential for various applications, ranging from scientific research, management, and public policy to the implementation of projects. However, the high processing cost required by DTM-LiDAR has led to the need to degrade spatial resolution. Therefore, it is crucial to understand how the coarsening of spatial resolution affects information loss in DTM-LiDAR. Additionally, identifying patterns of information loss is of great importance to guide future work with this type of data.

Hence, the objective of this study is to assess the effects caused by the coarsening of DTM's spatial resolution on topographic representations and drainage networks derived from DTM-LiDAR with a spatial resolution of 1 meter. The study area is a sub-basin of the Sirinhaem River watershed, located in the state of Pernambuco. Three resampling techniques and five spatial resolutions are employed for this purpose.

Material and Methods

Study Area Characteristics

The study area encompasses a sub-basin within the Sirinhaem River watershed, with an approximate area of 550 km². This sub-basin was selected due to the availability of 1-meter spatial resolution DTM-LiDAR data and compatibility with the computational capacity of the equipment used in this study. Figure 1 illustrates the study area.

This area faces water security issues (APAC, 2020), experiencing irregularities in annual precipitation and a trend of a 50% decrease in total annual precipitation. Additionally, it is prone to flooding events (Silva et al., 2017; Ferraz, 2019). Therefore, given these characteristics, the watershed requires hydrological studies focused on water resource management.

General Approach

The methodology employed in this study followed five main stages. The first stage involved the collection and preparation of DTM data. In the second stage, a resampling procedure was carried out, degrading the spatial resolution of the reference DTM to resolutions of 2, 10, 30, and 100 meters.

The third stage consisted of extracting topographic representations present in the reference and resampled DTMs. In the fourth stage, processing was performed for each DTM to characterize drainage networks and watersheds. Finally, metrics of evaluation were applied to the

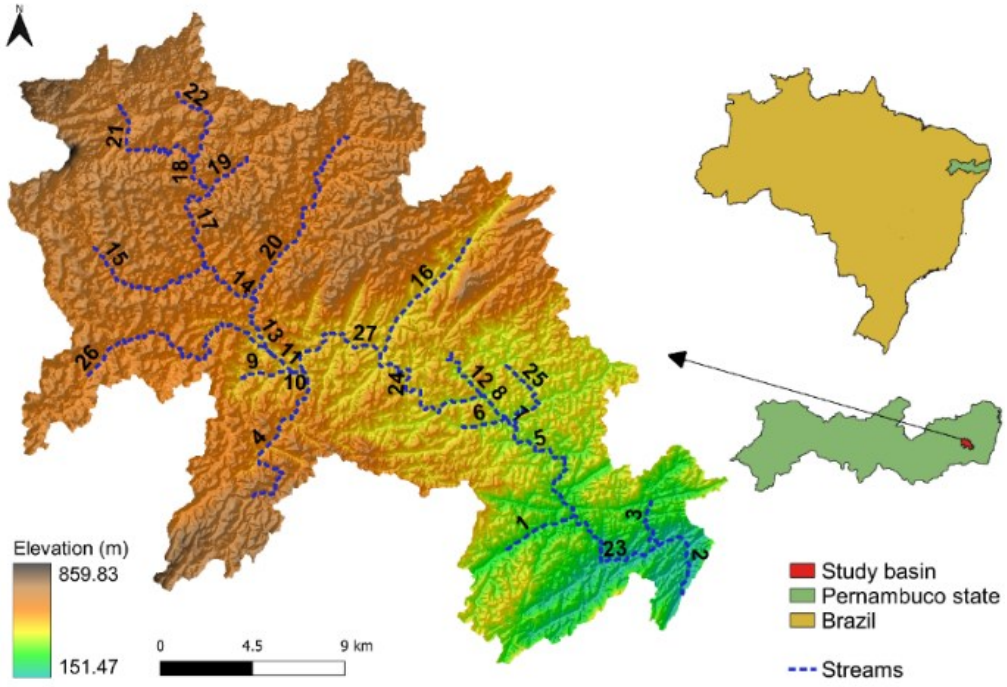

Figure 1. Location of the study area and reference drainage network with coding of river segments.

information plans extracted in the third and fourth stages.

To facilitate the understanding of the methodology sequence and results, Table 1 was created. It includes the coding adopted for the products extracted from the DTMs used in this research. The codes are based on the resampling technique and spatial resolution of the DTM, except for the reference DTM, which is coded as 'Reference' and is not included in the table.

Table 1. Coding adopted for products derived from resampled DTMs.

	Resampling technique		
Spatial resolution	**Mean aggregation**	**Bilinear interpolation**	**Nearest neighbor interpolation**
2 meters	MA2	BI2	NN2
10 meters	MA10	BI10	NN10
30 meters	MA30	BI30	NN30
100 meters	MA100	BI100	NN100

Collection and Preparation of DTM-LiDAR Data

For the construction of the reference DTM used in this study, 170 DTM-LiDAR scenes were utilized. These scenes were acquired through the Pernambuco Tridimensional program (PE3D) portal. The DTM-LiDAR scenes provided by PE3D have a spatial resolution of 1 meter at a 1:5000 scale, a radiometric resolution of 32 bits, and an altimetric precision better than 25 cm. They are referenced in the UTM Coordinate System, SIRGAS 2000 Datum, in the 25S zone for the study area. Each scene is approximately 33 megabytes, with 3,555 columns and 2,425 rows.

The PE3D aimed to conduct an aerophotogrammetric survey and laser profiling (LiDAR) of the entire territory of the state of Pernambuco, covering an area of 98,148 km² (Cirilo et al., 2014). The aerophotogrammetric coverage generated orthophotos at a 1:5000 scale with a spatial resolution of 50 cm, along with photo indices and respective metadata. The laser profiling had an approximate point density of 1 point per square meter, totaling about 50 billion points throughout the state (Cirilo et al., 2015).

In the DTM-LiDAR scenes used in this study, the presence of null elevation values was detected. To prevent potential error propagation in subsequent steps, the scenes underwent processing to eliminate null values. The procedure involved applying a filter to each DTM scene if null values were detected.

With the filtered scenes, the DTM-LiDAR scenes were concatenated, forming a single DTM-LiDAR file for the study area. The final result was a file composed of 170 scenes, generating a DTM with a spatial resolution of 1 meter, totaling 5.45 gigabytes, 41,860 columns, 34,979 rows, and a total of 1,464,220,940 pixels.

Resampling of the Reference DTM

The reference DTM-LiDAR (1 m spatial resolution) was resampled to resolutions of 2, 10, 30, and 100 meters. The choice of 2 and 10-meter resolutions is due to their ability to preserve a certain level of detail and, therefore, can be used in works that require higher levels of detail. The 30 and 100-meter resolutions were chosen for their suitability in projects involving large areas (Erdbrugger et al., 2021).

For resampling, three techniques were employed: mean aggregation, bilinear interpolation, and nearest neighbor interpolation. The selection of these resampling techniques is based on their well-established and extensive use in studies that investigated the effects of changing spatial resolution of DTMs (Sliwinski et al., 2022). Moreover, these methods are the most commonly used in the literature for resampling DTMs (Le Coz et al., 2009; Gillin et al., 2015; Muthusamy et al., 2021), having demonstrated satisfactory results.

Extraction of Topographic Representations

The topographic representations considered were the hypsometric curve and cross-sectional topographic profile (CTP). The analysis of these representations aimed to identify the pattern of information loss associated with the process of changing spatial resolution.

The cross-sectional topographic profile is commonly used in the literature to assess the difference between elevation data from DTMs with different sources and spatial resolutions (Vaze et al., 2010; Zhang et al., 2019). For this study, three CTPs were utilized, one in the upper portion, another in the middle, and the last one in the lower portion of the watershed. These locations were chosen because they represent zones with distinct elevation amplitudes.

Removal of Spurious Depressions in DTMs

The studied DTMs were processed to remove spurious depressions. This procedure is necessary to form continuous water flow lines, allowing for more realistic estimates of flow channel locations (Lidberg et al., 2017). For this procedure, the Fill Sinks XXL algorithm (Wang & Liu, 2006) was employed. This algorithm was chosen because it was designed to process high-resolution DTMs, presenting good computational efficiency in handling DTMs derived from LiDAR technology.

Calculation of Flow Directions and Accumulated Drainage Areas

Flow directions were computed using the Flow Accumulation (Top-Down) algorithm in SAGA GIS, employing the Deterministic 8 - D8 method (O'callaghan & Mark, 1984). This algorithm performs the simultaneous calculation of flow directions and accumulated drainage areas.

The D8 algorithm was chosen for this study as it is one of the most widely used for hydrological studies, offering simplicity and acceptable representation for conditions of unidirectional flow. Additionally, it ensures consistency between flow patterns, calculation of accumulated areas, and watershed delineation (Ariza-Villaverde et al., 2015).

Determination of Drainage Networks

To determine the drainage network, a minimum area value of 10 km² was adopted, and this value was used for all DTM datasets. The selection of the minimum area value was based on tests with the aim of avoiding the generation of a dense network, i.e., with many flow paths. A dense network increases the complexity of evaluation without necessarily contributing significantly to the purpose of this research.

The reference network adopted in this study is derived from the 1m DTM-LiDAR and consists of 27 segments, comprising segments of the main river and its tributaries. The analyses conducted in this research were performed considering the main river and the 27 segments, totaling 28 objects of analysis. Figure 1 shows the reference drainage network and the coding of the segments.

Watershed Delineation

In delineating the watershed, the choice of the outlet location took into consideration a limit on the drainage area to ensure that the computer used in this study could handle the processing. The location was based on the presence of a river monitoring point on the Sirinhaem River, which could contribute data for future studies. The outlet used for each resampled DTM was positioned at the same location or as close as possible to the reference outlet.

Application of Evaluation Metrics

Comparison of Cross-Sectional Topographic Profiles (CTP) – the comparison of CTPs aimed to identify the difference in elevation values in specific segments of the watershed between the reference DTM and the resampled DTMs. This comparison allowed for the identification and measurement of the loss of topographic representation caused by the change in spatial resolution.

Relative Variation of Hypsometric Curves – this metric aimed to assess the difference in elevations across the watershed as a percentage of the area. It allows us to examine the variation between elevation values in the resampled DTMs compared to the reference values (1m spatial resolution). Identifying the relative variation is crucial as it enables the quantification of information loss in topographic data during DTM resampling.

$$RV = \frac{(Res.E - Ref.E) * 100}{Ref.E} \quad (1)$$

Where:

RV – Relative variation of hypsometric curves;

Res.E – Resampled elevation (m);

Ref.E – Reference elevation (m).

Visual Inspection of Drainage Networks – visual inspection can be applied to both raster and vector drainage network files and is commonly used to assess network connectivity and identify topological and geometric errors (Polidori & El Hage, 2020). In this study, vector representations of drainage networks were analyzed by comparing the reference network (derived from the 1m DTM) with networks derived from resampled DTMs. The procedure involved overlaying the reference network outlines with those of the networks derived from resampled DTMs. This approach allowed for the assessment of the similarity

between network outlines and the identification of any errors present.

Average Distance Between Drainage Network Traces – this metric aims to quantify the degree of separation between drainage network traces by calculating the average distance between the traces of the reference network and those of the networks derived from resampled DTMs (Davies & Bell, 2009). For this study, the average distance between the drainage networks of resampled DTMs and the reference network was analyzed. The average distance was calculated as follows: the area of all polygons formed between the network traces was calculated, and then this result was divided by the length of the main river in the reference network (Chen et al., 2012).

Quantification of Streams Lengths – after calculating the lengths of the analyzed segments, a comparison was made between the reference and resampled values to assess whether there was an increase or decrease in length. The relative difference was calculated for the comparison.

$$RD = \frac{(Res.L - Ref.L) * 100}{Ref.\,L} \quad (2)$$

Where:

RD – Relative difference between stream lengths;

Res.L – Resampled length;

Ref.L – Reference length.

Percentage Within Buffer (PWB) – this evaluation metric estimates the percentage of a given drainage network that lies within a buffer generated around the reference network (Davies & Bell, 2009). The estimation is based on calculating the ratio between the sum of river segments within the buffer and the total length of that river. The result of the ratio is then multiplied by 100.

The selected buffer size should ensure that approximately 50% of the degraded DTM network is within the buffer region. This is because a very low buffer value would exclude a significant portion of the analyzed network, while a high value would include almost the entire network, making comparisons and analyses challenging (Davies & Bell, 2009).

In this study, each degraded spatial resolution drainage network was evaluated concerning the reference network. A buffer with a size of ½ pixel of the resampled DTM spatial resolution was applied to the object of analysis. According to De Sousa and Paz (2017), this buffer size ensures more balanced results, i.e., it is not too stringent to exclude a large portion of the network within the buffer and not too generous, allowing a large percentage within the buffer.

Watershed Delineation – this metric's primary role is to identify areas that are correctly delineated, erroneously omitted (omission error), and erroneously included (commission error) among the analyzed watersheds (De Sousa & Paz, 2017). This allows for the quantification of the percentage of these areas for the watersheds delineated from resampled DTMs compared to the reference watershed delineation (derived from the 1m DTM).

Quantification of Computational Cost – this metric assessed the extent to which the coarsening of spatial resolution led to a reduction in computational cost, measured in terms of disk storage space and algorithm processing time. The processing time of the Fill Sinks XXL, Flow Accumulation, and Channel Network algorithms in the SAGA GIS software was quantified. The storage space required by the files generated by these algorithms was also quantified for both the reference spatial resolution and degraded spatial resolutions.

Data computation followed some precautions. Firstly, the SAGA GIS software was kept open and running without parallel processing. Secondly, three processing rounds were performed for each algorithm, with the software closed and restarted at the beginning of each new round. The third precaution involved the individual evaluation of each time, discarding outlier values. If detected, a new round was conducted. At the end of the rounds, the average processing times for each algorithm were calculated.

The computer configuration used for data processing is as follows: Intel Core i5-8250U 1.60 GHz quad-core processor, 20 GB RAM, NVIDIA GeForce MX110 2 GB dedicated graphics card.

Results and discussions

Comparison of Cross-Sectional Topographic Profiles (CTP) – the CTPs are situated in distinct zones within the watershed and have different elevation ranges. CTP1 is located in the upper part of the watershed, CTP2 is in the middle portion, and CTP3 is in the lower portion. No significant effects on cross-sectional topographic profiles were observed due to changes in spatial resolutions when comparing the reference

CTPs with those derived from degraded resolutions.

Resolutions of 2 and 10 meters showed relatively small differences, not exceeding 4 meters. The 30-meter resolution exhibited slight differences, mainly in peaks, which could reach up to 8 meters in certain segments. The 100-meter spatial resolution showed larger differences compared to the others. Additionally, it demonstrated difficulties in representing elevation variations over short distances and exhibited peaks and valleys that were displaced and generally smaller.

These results align with other studies (Vaze et al., 2010; Sliwinski et al., 2022;) exploring the change in spatial resolution in LiDAR-derived CTPs. In these studies, coarser resolutions face challenges in representing elevation changes over short distances and show displacements of peaks and valleys.

Analysis of Hypsometric Curves – for the hypsometric curves of all degraded spatial resolutions, no significant differences were identified compared to the reference curve. This demonstrates that, despite the information being degraded up to 100 times, the hypsometric characterization practically remains unchanged. This finding is consistent with the work of Mendonça and Paz (2022), where they show no significant differences between hypsometric curves of resampled LiDAR-derived DTMs at resolutions of 2, 10, and 30 meters.

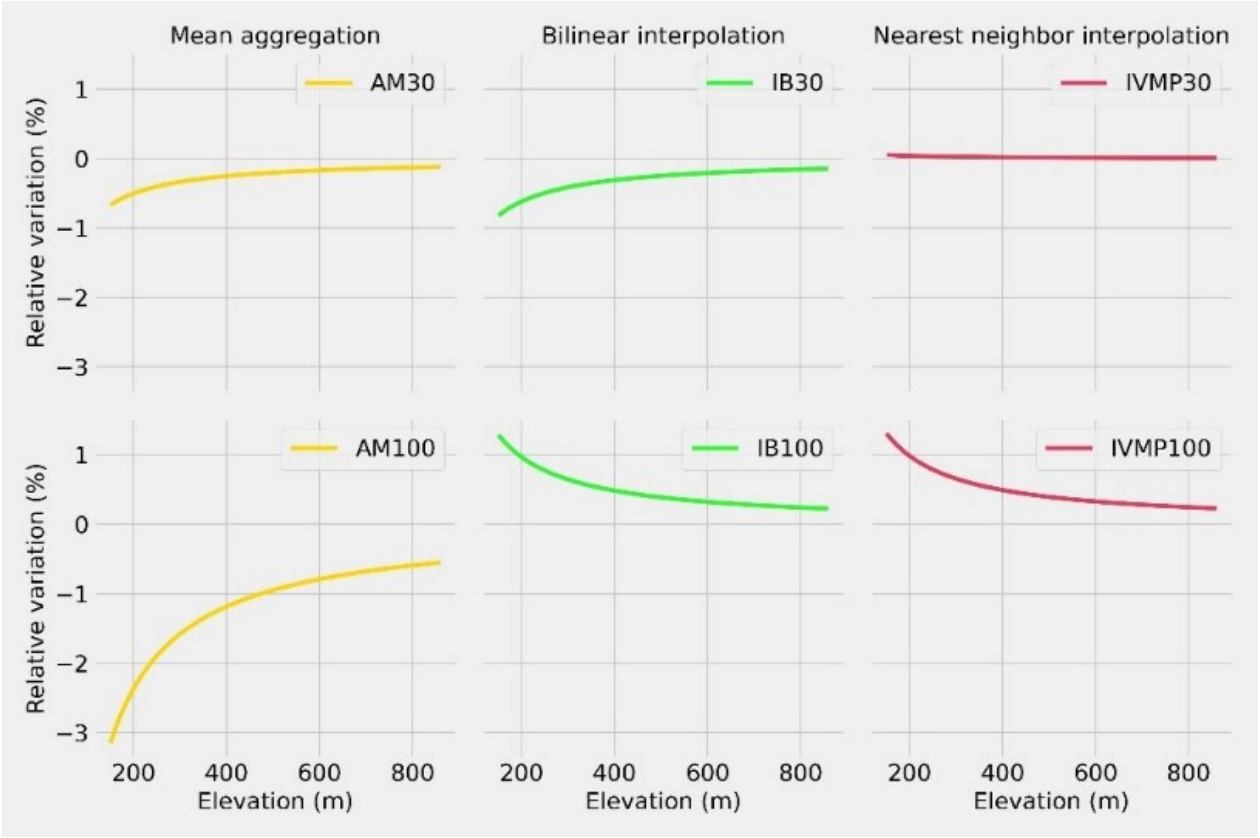

Figure 2. Relative variation of hypsometric curves: mean aggregation (MA), bilinear interpolation (BI), and nearest neighbor interpolation (NN) at resolutions of 30 and 100 meters.

Analyzing the relative variations of the hypsometric curves reveals a pattern of increasing variation at lower elevations. This pattern is observed for all three resampling methods and at all degraded resolutions. In all resampling methods, resolutions of 2 and 10 meters exhibited nearly identical behavior, with a maximum relative variation of less than 0.08%. Meanwhile, for resolutions of 30 and 100 meters, the highest variations were -0.82% and -3.15%, respectively. Figure 2 illustrates the relative variation of hypsometric curves.

Visual Inspection of Drainage Networks – in general, visual inspection reveals that when analyzing drainage networks from resampled DTMs with the same spatial resolution, there are no significant relative differences between them. However, a higher similarity in traces is observed between networks generated by DTMs resampled

using bilinear interpolation and nearest neighbor interpolation methods.

However, when analyzing networks derived from DTMs resampled at different spatial resolutions, it is generally observed that the spatial resolution showing the highest similarity with the reference network (1 meter) is 2 meters, followed by 10, 30, and 100 meters.

Through visual inspection of drainage networks, it was observed that as the degree of spatial resolution coarsening increases, the drainage networks show greater distancing and displacement of confluences compared to the reference network. This tends to result in both an increase and a decrease in the length of segments. Additionally, the networks also lost the ability to represent meanders, which can lead to the underestimation of length for most segments.

These findings are consistent with the results of other studies (Vaze et al., 2010; Yang et al., 2014; Souza & Paz, 2017; Mendonça & Paz, 2022;), which emphasize that the higher the degree of spatial resolution coarsening, the greater the effects of resolution change on drainage networks. Figure 3 illustrates segments of the reference drainage network and networks derived from resampled DTMs.

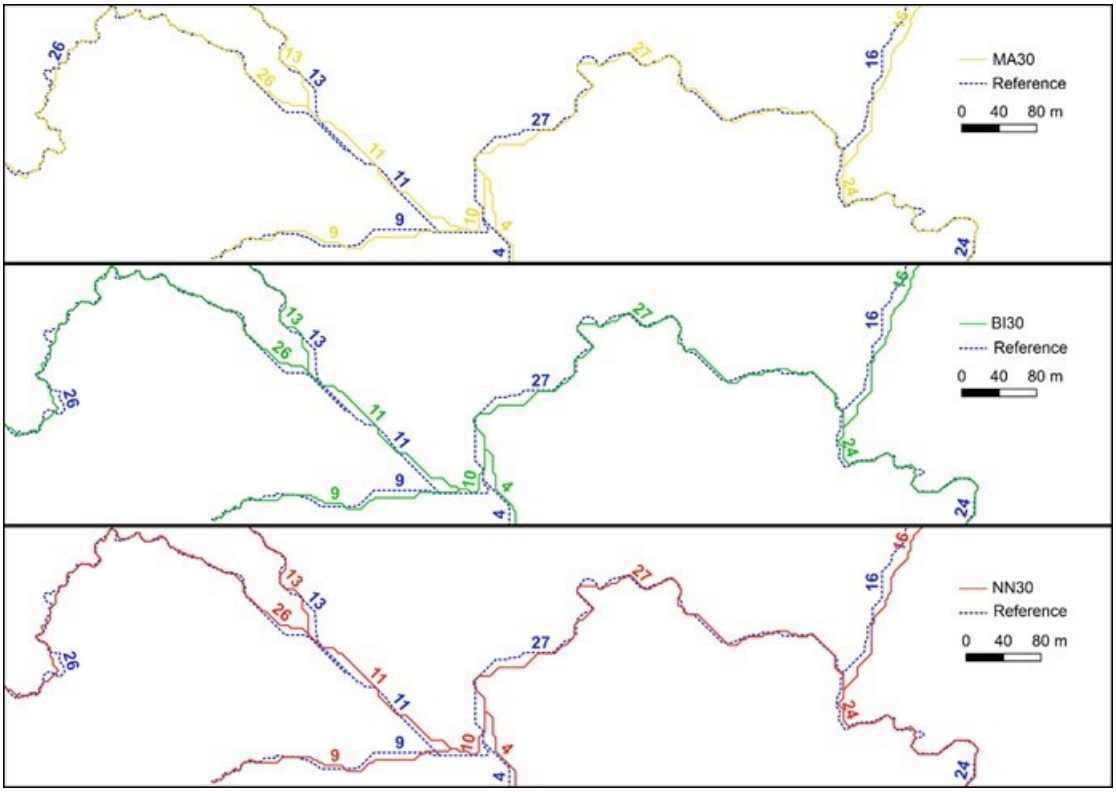

Figure 3. Tracings of drainage networks at the confluence of segments 13 and 26, 9 and 11, 10 and 4, 27 and 16: for reference networks and resampled networks at a spatial resolution of 30 meters.

Mean Distance – the evaluation of the mean distance between the reference network and the degraded MDT networks showed that for the same spatial resolution, the distance value was very close between the networks. No significant differences were identified between the resampling techniques.

Moreover, it was noted that with the increase in spatial resolution coarsening, the mean distance tends to increase. Furthermore, the displacement of confluences was a determining factor in the result of the average distance calculation, favoring the generation of larger values.

These findings align with the results of other studies (Chen et al., 2012; De Sousa & Paz, 2017), which show that when spatial resolution is degraded, drainage networks tend to lose precision. In a method that assesses the error in the distance between drainage networks, Yang et al. (2014) demonstrate that for coarser resolutions, the error increases, meaning that the distance between networks is greater as the resolution is coarsened.

Figure 4 illustrates the average distance of the main river.

Stream Lengths – upon obtaining the lengths of the main river and its segments, the relative differences between the lengths of the reference network segments and those derived from resampled DTM networks were analyzed. It was observed that, in general, most segments in all degraded networks exhibited a pattern of underestimating length. Various studies (Goulden et al., 2014; Yang et al., 2014; Souza & Paz, 2017; Mendonça & Paz, 2022; Sliwinski et al., 2022;) have also concluded that the coarsening of spatial resolution leads to a decrease in the length of flow paths.

Sliwinski et al. (2022) tested six resampling techniques, and all of them resulted in a reduction in the length of flow paths. The findings of Yang et al.'s work (2014) also indicate a reduction in the total length of rivers. For a spatial resolution of 10 meters, there was a relative difference of approximately 10%, and for a resolution of 30 meters, the relative difference reaches up to 16%.

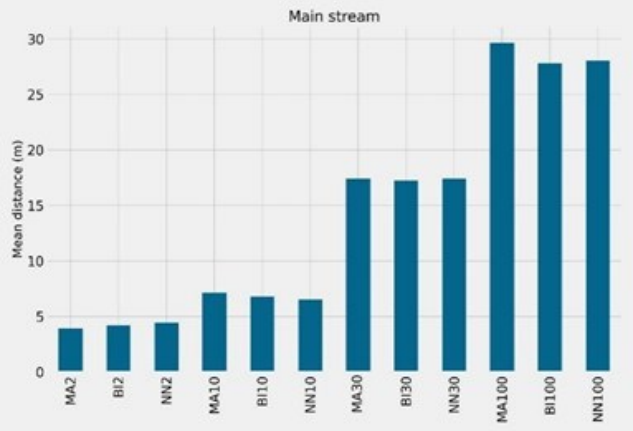

Figure 4. Mean distance between main rivers for resampling methods: mean aggregation (MA), bilinear interpolation (BI), and nearest neighbor interpolation (NN) at resolutions of 2, 10, 30, and 100 meters.

As a general trend, the results of Yang et al. (2014) for spatial resolutions of 5 and 10 meters are similar to those found in this research. However, for a spatial resolution of 30 meters, the results do not follow the same pattern, although some segments in this study exhibit a pattern close to the results of the cited authors.

In the work of De Sousa and Paz (2017), the proportion of spatial resolution coarsening jump was similar, ranging from 1 km to 5, 10, 20, and 30 km. The results show that the relative differences were higher than 30% for most analyzed river lengths. This indicates that for the same proportion of spatial resolution coarsening, differences greater than those found in this study were observed for resolutions 10 and 30 times larger.

The displacement of confluences was a determining factor for the difference in segment lengths, causing an increase in some segments and a decrease in others. Another important factor was the reduction in the ability to accurately represent meanders, leading to a decrease in segment lengths. This occurs due to the increase in pixel size, which makes it challenging to perform precise delineation of meanders.

When evaluating which resampling technique presents segments with smaller relative differences, overall, interpolation by the nearest neighbor has a slight advantage. Therefore, despite there being a small difference in performance among the techniques, for the same spatial resolution, the methods yield similar results. Figure 5 illustrates the values of relative difference between the length of the main reference river and the main rivers in networks derived from resampled DTMs.

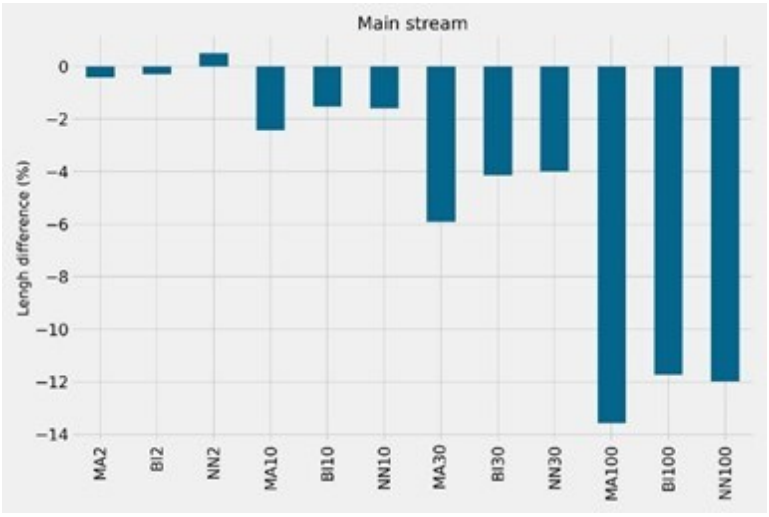

Figure 5. Relative length difference among main rivers for resampling methods: mean aggregation (MA), bilinear interpolation (BI), and nearest neighbor interpolation (NN) at resolutions of 2, 10, 30, and 100 meters.

Percentage Within Buffer (PWB) – in assessing the percentage within the buffer, a higher percentage indicates better quality of the traced drainage network under evaluation. Generally, results by spatial resolution show that the percentages for networks of the same resolution are close.

It is noted that the buffer size and the distance between the traced drainage networks are the factors that exerted the greatest influence on the percentage calculation. Consequently, it was observed that the 100-meter resolution exhibited higher PWB, followed by 2, 10, and 30 meters.

In contrast to the approach taken in this study, Goulden et al. (2014) used a different approach, adopting a fixed buffer size of 3 meters for the evaluation of different spatial resolutions. They observed that with the coarsening of spatial resolution, PWB decreased.

In the study by De Sousa and Paz (2017), when a buffer of half the size of the pixel of the degraded spatial resolution was adopted, there was a tendency for an increase in PWB for most analyzed rivers, especially for coarser resolutions. This aligns with the results found in this research. The PWB for the main rivers in this study is illustrated in Figure 6.

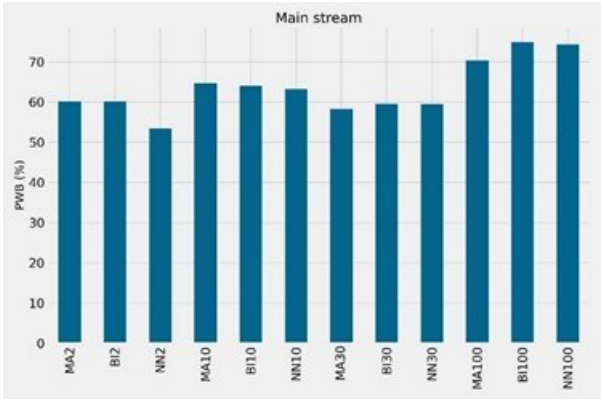

Figure 6. Percentage within buffer of the main river for resampling methods: mean aggregation (MA), bilinear interpolation (BI), and nearest neighbor interpolation (NN) at resolutions of 2, 10, 30, and 100 meters.

Watershed Delineation – trough the delineation of the watershed of the reference drainage network and those derived from resampled DTMs, it was possible to compute the percentage of concordance area, commission errors, and omission errors of the analyzed networks. Figure 8 illustrates the percentages of concordance, commission, and omission areas for each DTM.

The results show that the percentages of concordance area, commission error, and omission error among all networks are close to each other. Despite the proximity of the values, as the degree of coarsening of spatial resolution increases, the concordance values decrease, and commission and omission errors increase.

The variation in percentages for concordance and omission error was 1.76%, and for commission error, it was 0.948%. This indicates that even degrading the reference information up to 100 times, there are compensations of areas, allowing the watershed area value to be relatively accurate.

The 2-meter resolution achieved better results, followed by 10, 30, and 100 meters. Therefore, from the presented results, it is evident that the coarsening of spatial resolution leads to a decrease in the watershed area. This aligns with the findings of various studies in the literature (Goulden et al., 2014; Souza & Paz, 2017; Mendonça & Paz, 2022; Sliwinski et al., 2022;). The work of Mendonça and Paz (2022) shows percentage decreases of similar order of magnitude to the present study. Goulden et al. (2014) report that errors in watershed delineation found in their work are linked to the topographic characteristics of the terrain, elimination of hydrological features at coarser resolutions, and errors in LiDAR altimetric measurements due to vegetation.

On the other hand, other studies (Wu et al., 2008; Tan et al., 2015; Edbrugger et al., 2021) show that the change from finer to coarser spatial resolution resulted in an increase in watershed area.

Computational Cost – the resampling of the LiDAR-DTM resulted in an extreme reduction in algorithm processing time and disk storage space, reaching up to 5,031,900% and 986,394%, respectively. The variation in processing time for algorithms (Fill Sinks XXL, Flow Accumulation, and Channel Network) among spatial resolutions illustrates how the coarsening of spatial resolution reduces computational cost, which may be necessary when working with large areas.

Although processing time was not a prohibitive factor in this study, for larger areas with a consequently greater number of pixels, processing time and limitations in RAM memory can become prohibitive factors.

DTM	MA2 (%)	BI2 (%)	NN2 (%)	MA10 (%)	BI10 (%)	NN10 (%)	MA30 (%)	BI30 (%)	NN30 (%)	MA10 0 (%)	BI100 (%)	NN100 (%)
Agreement	99.80	99.95	99.94	99.80	99.80	99.75	99.49	99.50	99.49	98.60	98.20	99.17
Omission	0.19	0.05	0.06	0.19	0.19	0.25	0.51	0.51	0.51	1.4	1.81	1.81
Comission	0.13	0.04	0.05	0.13	0.13	0.12	0.52	0.22	0.21	0.92	0.96	0.99

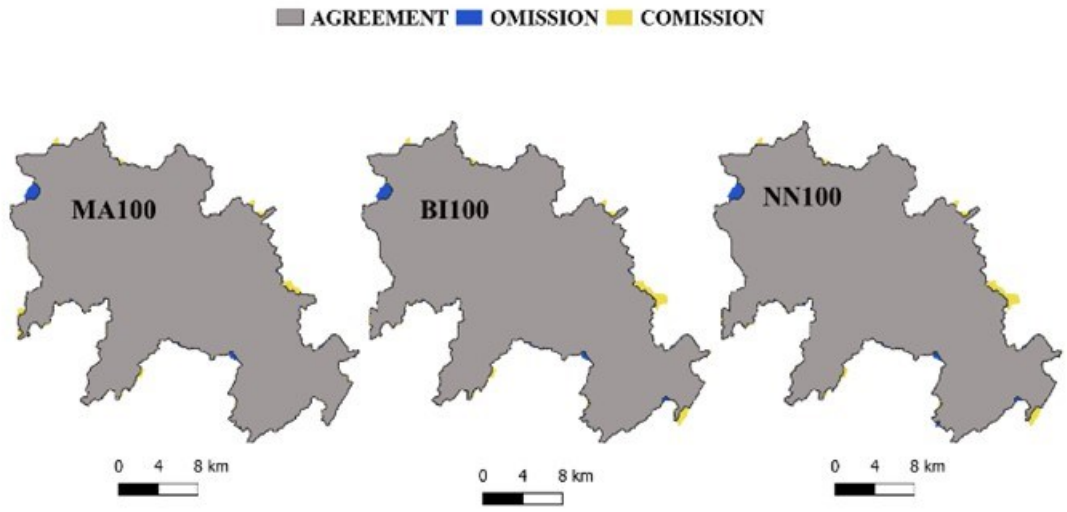

Figure 7. Computation of concordance, omission, and commission areas in watershed delineation: mean aggregation (MA), bilinear interpolation (BI), and nearest neighbor interpolation (NN) at resolutions of 2, 10, 30, and 100 meters.

Therefore, algorithms with more efficient processing have been proposed, reducing the computational processing cost. For example, algorithms utilizing parallel processing (Gong & Xie, 2009; Barnes et al., 2014; Yildirim et al., 2015; Stanislawski et al., 2018).

Regarding computational cost by spatial resolution, it is observed that for the three

resampling techniques, processing times were practically equal, with only slight variations of a few seconds. In terms of disk storage space, there is no variation in space between files of the same spatial resolution, as they have the same number of rows and columns and the same data type. This reinforces that in terms of computational cost, there are no significant differences between resampling techniques, but rather in relation to spatial resolutions.

The results show a significant reduction in processing time as the spatial resolution becomes coarser, which was expected due to the lower number of pixels to process. It can be noted that processing time goes from the scale of minutes for spatial resolutions of 1 and 2 meters to just a few seconds for resolutions of 10, 30, and 100 meters. When analyzing the reduction in time in relation to the previous resolution, it is evident that the reduction is also significant, but to a lesser extent compared to the reference resolution.

Figure 8 illustrates the processing time of algorithms by spatial resolution. It is possible to observe a significant decrease in processing time, especially from the 1 to 2-meter resolution. Additionally, the time for resolutions of 10, 30, and 100 meters is practically immediate. This can be explained by the quantity of pixels to be processed at these spatial resolutions, and thus, most of the processing time consists of initialization elements and fixed-time algorithm procedures, limiting a further reduction in processing time.

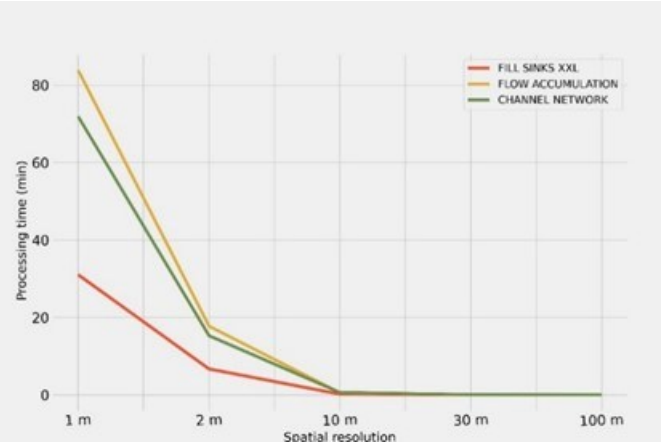

Figure 8. Algorithm processing time by spatial resolution.

The reduction in disk storage space and processing time is illustrated in Figure 9. The results show an exponential trend of increasing reductions in disk storage space and processing time with the coarsening of spatial resolution. Additionally, for the 2 and 100-meter resolutions, the greatest reduction was in the processing time of the Flow Accumulation algorithm, while for the 10 and 30-meter resolutions, it was in the processing of the Fill Sink XXL algorithm.

The results align with studies found in the literature. For example, in the study by Mendonça and Paz (2022), they also used the Fill Sinks XXL and Flow Accumulation algorithms in SAGA GIS and observed an extreme reduction in processing time and disk size. In another study, Metz et al. (2011), using different algorithms, also reported a significant reduction in processing time for coarser resolutions.

Conclusions

Based on the evaluations conducted, no significant differences were identified between the resampling techniques. However, resampling resulted in significant variations among the analyzed spatial resolutions. Topographic representations did not show relevant differences between spatial resolutions, except for the 100-meter spatial resolution meter spatial resolution.

DTM resampling led to confluence displacement, distancing from the reference drainage network, and a loss of the ability to represent meanders. These effects can lead to errors in generating other information layers, such as flood area estimation, sediment transport, or intersection with other types of data

Watershed delineation did not show significant information loss as the spatial resolution degraded. In terms of computational cost, a substantial reduction in processing time and disk storage space was identified due to DTM resampling.

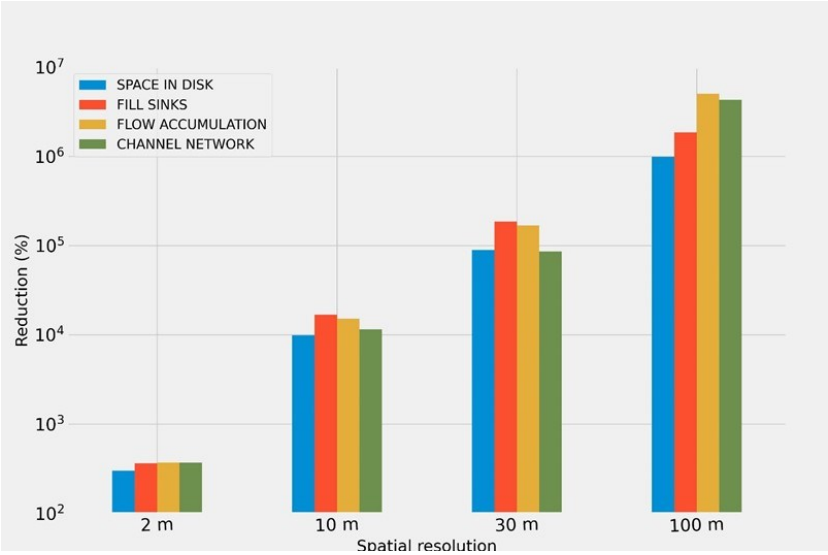

Figure 9. Reduction by spatial resolution of disk storage space and processing time for the Fill Sinks XXL, Flow Accumulation, and Channel Network algorithms in relation to the 1-meter spatial resolution.

Finally, the 2-meter spatial resolution yielded the best results. Therefore, this resolution is the most suitable in case of a need for data resampling for this study area, as it presented a significant reduction in computational cost without losing the representation of topographic features, quality of the drainage network trace, and watershed delineation.

Acknowledgment

Authors thanks to the CAPES (Coordenação de Aperfeiçoamento de Pessoal de Nível Superior - Brazil), for the master of science scholarship.

References

Agência Nacional de Águas e Saneamento Básico – ANA. (2022). Hidroweb: Sistemas de informações hidrológicas. Retrieved in 2022, September 11, from https://www.snirh.gov.br/hidroweb/

Agência Pernambucana de Águas e Clima - APAC. (2020). Atualização do plano estadual de recursos hídricos de Pernambuco – PERH|PE (diagnóstico integrado). Recife. Retrieved in 2022, September 14, from https://www.perhpe.com.br/downloads

Ariza-Villaverde, A. B., Jiménez-Hornero, F. J., & De Ravé, E. G. (2015). Influence of DEM resolution on drainage network extraction: A multifractal analysis. Geomorphology, 241, 243–254. https://doi.org/10.1016/j.geomorph.2015.03.040

Azizian, A., & Brocca, L. (2019). Determining the best remotely sensed DEM for flood inundation mapping in data sparse regions. International Journal of Remote Sensing, 41(5), 1884–1906. https://doi.org/10.1080/01431161.2019.1677968

Barnes, R., Lehman, C., & Mulla, D. J. (2014). Priority-flood: An optimal depression-filling and watershed-labeling algorithm for digital elevation models. Computers & Geosciences, 62, 117–127. https://doi.org/10.1016/j.cageo.2013.04.024

Chen, Y., Wilson, J. P., Zhu, Q.; & Zhou, Q., 2012. Comparison of drainage constrained methods for DEM generalization. Computers and Geosciences, 48, 41-49. https://doi.org/10.1016/j.cageo.2012.05.002

Cirilo, J. A., Alves, F. H. B., Silva, B. M., & Campos, P. H. A. L. C. (2015). Pernambuco tridimensional: base de dados espaciais para planejamento urbano e gestão territorial. In 12th Simpósio de Hidráulica e Recursos Hídricos dos Países de Expressão Portuguesa, Brasília. Retrieved in 2022, December 12, from https://anais.abrhidro.org.br/job.php?Job=12751.

Cirilo, J. A., Alves, F. H. B., Da Silva, L. a. C., & De Andrade Lima Campos, J. H. (2014). Suporte de Informações Georreferenciadas de Alta Resolução para Implantação de Infraestrutura e Planejamento Territorial (Support of Georeferenced Information of High Resolution for Implementation of Infrastructure and Territorial Planning). Revista Brasileira De Geografia Física, 7(4), 755–763. https://doi.org/10.26848/rbgf.v7.4.p755-763

Davies, H., & Bell, V. A. (2009). Assessment of methods for extracting low-resolution river networks from high-resolution digital data.

Hydrological Sciences Journal, 54(1), 17–28. https://doi.org/10.1623/hysj.54.1.17

Erdbrügger, J., Van Meerveld, I., Bishop, K., & Seibert, J. (2021). Effect of DEM-smoothing and -aggregation on topographically-based flow directions and catchment boundaries. Journal of Hydrology, 602, 126717. https://doi.org/10.1016/j.jhydrol.2021.126717

Ferraz, G. F. (2019). Simulação hidrológica e hidrodinâmica do impacto de enchentes na bacia do rio Sirinhaém e avaliação de sistema de controle proposto. [Master's thesis, Universidade Federal de Pernambuco]. UFPE Repository. Retrieved in 2022, September 18, from https://repositorio.ufpe.br/handle/123456789/34017

Gillin, C. P., Bailey, S. W., McGuire, K. J., & Prisley, S. P. (2015). Evaluation of Lidar-derived DEMs through Terrain Analysis and Field Comparison. Photogrammetric Engineering and Remote Sensing, 81(5), 387–396. https://doi.org/10.14358/pers.81.5.387.

Gong, J., & Xie, J. (2009). Extraction of drainage networks from large terrain datasets using high throughput computing. Computers & Geosciences, 35(2), 337–346. https://doi.org/10.1016/j.cageo.2008.09.002

Goulden, T., Hopkinson, C., Jamieson, R., & Sterling, S. (2014). Sensitivity of watershed attributes to spatial resolution and interpolation method of LiDAR DEMs in three distinct landscapes. Water Resources Research, 50(3), 1908–1927. https://doi.org/10.1002/2013wr013846.

Grohmann, C. H. (2015). Effects of spatial resolution on slope and aspect derivation for regional-scale analysis. Computers & Geosciences, 77, 111–117. https://doi.org/10.1016/j.cageo.2015.02.003.

Habtezion, N., Nasab, M. T., & Chu, X. (2016). How does DEM resolution affect microtopographic characteristics, hydrologic connectivity, and modelling of hydrologic processes? Hydrological Processes, 30(25), 4870–4892. https://doi.org/10.1002/hyp.10967.

Coz, M. L., Dagognet, F., Genthon, P., & Favreau, G. (2009). Assessment of Digital Elevation Model (DEM) aggregation methods for hydrological modeling: Lake Chad basin, Africa. Computers & Geosciences, 35(8), 1661–1670. https://doi.org/10.1016/j.cageo.2008.07.009.

Lidberg, W., Nilsson, M., Lundmark, T., & Ågren, A. (2017). Evaluating preprocessing methods of digital elevation models for hydrological modelling. Hydrological Processes, 31(26), 4660–4668. https://doi.org/10.1002/hyp.11385.

Lindsay, J. B., & Creed, I. F. (2005). Sensitivity of digital landscapes to artifact depressions in remotely-sensed DEMs. Photogrammetric Engineering and Remote Sensing, 71(9), 1029–1036. https://doi.org/10.14358/pers.71.9.1029.

Lindsay, J. B., Francioni, A., & Cockburn, J. M. H. (2019). LIDAR DEM smoothing and the preservation of drainage features. Remote Sensing, 11(16), 1926. https://doi.org/10.3390/rs11161926.

Lisenby, P. E., & Fryirs, K. (2017). 'Out with the Old?' Why coarse spatial datasets are still useful for catchment-scale investigations of sediment (dis)connectivity. Earth Surface Processes and Landforms, 42(10), 1588–1596. https://doi.org/10.1002/esp.4131.

Meles, M. B.; Younger, S. E.; Jackson, C. R.; Du, E.H.; & Drover, D.T. (2020). Wetness index based on landscape position and topography (WILT): Modifying TWI to reflect landscape position. Journal of Environmental Management, 225, 109863. https://doi.org/10.1016/j.jenvman.2019.109863

Mendonça, R. L.; & Paz, A. R. (2022). LiDAR data for topographical and river drainage characterization: capabilities and shortcomings. Revista Brasileira de Recursos Hídricos, 27. https://doi.org/10.1590/2318-0331.272220220092

Metz, M., Mitášová, H., & Harmon, R. S. (2011). Efficient extraction of drainage networks from massive, radar-based elevation models with least cost path search. Hydrology and Earth System Sciences, 15(2), 667–678. https://doi.org/10.5194/hess-15-667-2011.

Muhadi, N. A., Abdullah, A. F., Bejo, S. K., Mahadi, M. R., & Mijic, A. (2020). The Use of LiDAR-Derived DEM in Flood Applications: A review. Remote Sensing, 12(14), 2308. https://doi.org/10.3390/rs12142308.

Muthusamy, M., Casado, M. R., Butler, D., & Leinster, P. (2021). Understanding the effects of Digital Elevation Model resolution in urban fluvial flood modelling. Journal of Hydrology, 596, 126088. https://doi.org/10.1016/j.jhydrol.2021.126088.

O'Callaghan, J., & Mark, D. (1984). The extraction of drainage networks from digital elevation data. Computer Vision, Graphics, and Image Processing, 28(3), 323–344. https://doi.org/10.1016/s0734-189x(84)80011-0.

Persendt, F., & Gomez, C. (2016). Assessment of drainage network extractions in a low-relief

area of the Cuvelai Basin (Namibia) from multiple sources: LiDAR, topographic maps, and digital aerial orthophotographs. Geomorphology, 260, 32–50. https://doi.org/10.1016/j.geomorph.2015.06.047.

Polidori, L., & Hage, M. E. (2020). Digital Elevation Model Quality Assessment Methods: A Critical review. Remote Sensing, 12(21), 3522. https://doi.org/10.3390/rs12213522.

Roostaee, M., & Deng, Z. (2022). Effects of digital elevation model data source on HSPF-based watershed-scale flow and water quality simulations. Environmental Science and Pollution Research, 30(11), 31935–31953. https://doi.org/10.1007/s11356-022-24449-9.

Da Silva, R. O. B., Montenegro, S. M. G. L., & De Souza, W. M. (2017). Tendências de mudanças climáticas na precipitação pluviométrica nas bacias hidrográficas do estado de Pernambuco. Engenharia Sanitaria E Ambiental, 22(3), 579–589. https://doi.org/10.1590/s1413-41522017142481.

Śliwiński, D., Konieczna, A., & Roman, K. (2022). Geostatistical resampling of LIDAR-Derived DEM in wide resolution range for modelling in SWAT: A case study of Zgłowiączka River (Poland). Remote Sensing, 14(5), 1281. https://doi.org/10.3390/rs14051281.

Sørensen, R., & Seibert, J. (2007). Effects of DEM resolution on the calculation of topographical indices: TWI and its components. Journal of Hydrology, 347(1–2), 79–89. https://doi.org/10.1016/j.jhydrol.2007.09.001.

De Sousa, T. M. I., & Da Paz, A. R. (2017). How to evaluate the quality of coarse-resolution DEM-derived drainage networks. Hydrological Processes, 31(19), 3379–3395. https://doi.org/10.1002/hyp.11262.

Stanislawski, L. V., Survila, K., Wendel, J., Liu, Y., & Buttenfield, B. P. (2017). An open source high-performance solution to extract surface water drainage networks from diverse terrain conditions. Cartography and Geographic Information Science, 45(4), 319–328. https://doi.org/10.1080/15230406.2017.1337524.

Tan, M. L., Ficklin, D. L., Dixon, B. M., Ibrahim, A. L., Yusop, Z., & Chaplot, V. (2015). Impacts of DEM resolution, source, and resampling technique on SWAT-simulated streamflow. Applied Geography, 63, 357–368. https://doi.org/10.1016/j.apgeog.2015.07.014.

Vaze, J., Teng, J., & Spencer, G. (2010). Impact of DEM accuracy and resolution on topographic indices. Environmental Modelling and Software, 25(10), 1086–1098. https://doi.org/10.1016/j.envsoft.2010.03.014.

Wang, L., & Liu, H. (2006). An efficient method for identifying and filling surface depressions in digital elevation models for hydrologic analysis and modelling. International Journal of Geographical Information Science, 20(2), 193–213. https://doi.org/10.1080/13658810500433453.

Winzeler, H., Owens, P. R., Read, Q. D., Libohova, Z., Ashworth, A. J., & Sauer, T. J. (2022). Topographic Wetness Index as a proxy for soil moisture in a Hillslope catena: Flow algorithms and map Generalization. Land, 11(11), 2018. https://doi.org/10.3390/land11112018.

Woodrow, K., Lindsay, J. B., & Berg, A. (2016). Evaluating DEM conditioning techniques, elevation source data, and grid resolution for field-scale hydrological parameter extraction. Journal of Hydrology, 540, 1022–1029. https://doi.org/10.1016/j.jhydrol.2016.07.018.

Wu, S., Li, J., & Huang, G. (2008). A study on DEM-derived primary topographic attributes for hydrologic applications: Sensitivity to elevation data resolution. Applied Geography, 28(3), 210–223. https://doi.org/10.1016/j.apgeog.2008.02.006.

Yang, J., & Chu, X. (2013). Effects of DEM resolution on surface depression properties and hydrologic connectivity. Journal of Hydrologic Engineering, 18(9), 1157–1169. https://doi.org/10.1061/(asce)he.1943-5584.0000731.

Yang, P., Ames, D. P., Fonseca, A., Anderson, D., Shrestha, R., Glenn, N. F., & Cao, Y. (2014). What is the effect of LiDAR-derived DEM resolution on large-scale watershed model results? Environmental Modelling and Software, 58, 48–57. https://doi.org/10.1016/j.envsoft.2014.04.005.

Yıldırım, A. A., Watson, D., Tarboton, D. G., & Wallace, R. M. (2015). A virtual tile approach to raster-based calculations of large digital elevation models in a shared-memory system. Computers & Geosciences, 82, 78–88. https://doi.org/10.1016/j.cageo.2015.05.014.

Zhang, K., Gann, D., Ross, M. S., Robertson, Q., Sarmiento, J. P., De Santana, S. A., Rhome, J., & Fritz, C. (2019). Accuracy assessment of ASTER, SRTM, ALOS, and TDX DEMs for Hispaniola and implications for mapping vulnerability to coastal flooding. Remote Sensing of Environment, 225, 290–306. https://doi.org/10.1016/j.rse.2019.02.028.